Liquid Crystals

ISSN: 0267-8292 (Print) 1366-5855 (Online) Journal homepage: www.tandfonline.com/journals/tlct20

Ageing of thermomechanical and elastocaloric response of liquid crystalline elastomers

Matic Morgan , Andraž Rešetič , Zdravko Kutnjak & Brigita Rožič

To cite this article: Matic Morgan , Andraž Rešetič , Zdravko Kutnjak & Brigita Rožič (05 Aug 2026): Ageing of thermomechanical and elastocaloric response of liquid crystalline elastomers, Liquid Crystals, DOI: 10.1080/02678292.2026.2712559

To link to this article: https://doi.org/10.1080/02678292.2026.2712559

Published online: 05 Aug 2026.

LIQUID CRYSTALS
https://doi.org/10.1080/02678292.2026.2712559

Ageing of thermomechanical and elastocaloric response of liquid crystalline elastomers

Matic Morgan[a,b], Andraž Rešetič[a], Zdravko Kutnjak[a,b] and Brigita Rožič[a,b]

[a]Condensed Matter Physics Department, Jožef Stefan Institute, Ljubljana, Slovenia; [b]Jožef Stefan Postgraduate School, Ljubljana, Slovenia

ABSTRACT

Main-chain liquid-crystalline elastomers were examined to assess their long-term thermomechanical stability and elastocaloric performance under repeated uniaxial actuation. The monodomain samples, prepared with tunable crosslink densities and well – defined nematic – isotropic (N–I) transitions, were subjected to up to 1,000,000 stretch – retract cycles using a custom extensometer capable of simultaneous strain, stress, and temperature measurements. Relatively small mechanical fatigue and absence of cracking and delamination were observed throughout the test duration, demonstrating excellent mechanical resilience. Repeated cycling produced a gradual enhancement of the elastocaloric temperature change, reaching a steady-state increase after several thousand cycles, consistent with stress-induced stabilisation of mesogenic alignment. Concurrently, the N-I transition temperature decreased by approximately 13 K, indicating partial network relaxation and reorganisation under prolonged loading. These results show that cyclic actuation can improve elastocaloric responsiveness while preserving structural integrity, highlighting MC-LCEs as robust and sustainable candidates for next-generation solid-state heat-management technologies.

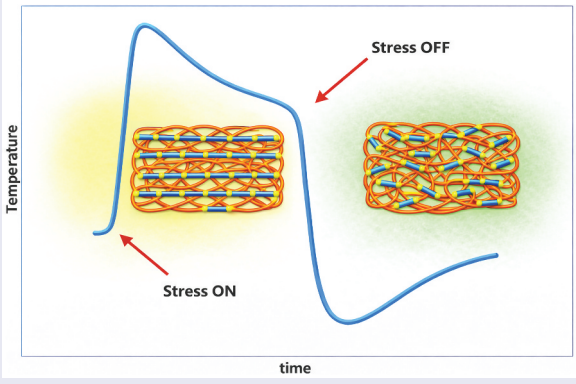

ARTICLE HISTORY
Received 26 March 2026
Accepted 27 July 2026

KEYWORDS
Liquid-crystalline elastomers; elastocaloric effect; mechanical ageing; solid-state cooling; heat management

1. Introduction

The growing global demand for cooling and refrigeration presents an increasingly urgent environmental challenge. Conventional vapour compression systems rely on high-global-warming-potential refrigerants and consume substantial electrical energy, contributing significantly to greenhouse gas emissions [1–4]. These concerns have intensified the search for alternative solid-state cooling technologies based on caloric effects, in which a material undergoes a reversible temperature change when an external field – magnetic, electric, hydrostatic, or mechanical – is applied or removed [2,5–11]. Among these, the elastocaloric effect (eCE), driven by mechanical stress, has emerged as a particularly promising route towards efficient and environmentally friendly cooling devices or heat pumps [12–17].

Traditional elastocaloric materials, such as shape-memory alloys (SMAs), can exhibit very large temperature changes, reaching up to 40 K under high applied stresses [1,2,12,14,15,18,19]. However, their practical deployment is hindered by the need for extremely large stress fields (hundreds of MPa to nearly 1 GPa), mechanical fatigue, and the complexity of the required actuation hardware. These limitations motivate the exploration of soft mechanocaloric materials, such as

CONTACT Brigita Rožič brigita.rozic@ijs.si

liquid-crystalline elastomers (LCEs), where comparable entropy changes can be achieved at stress levels orders of magnitude lower.

Liquid-crystalline elastomers have recently attracted attention as a compelling class of soft elastocaloric materials. LCEs combine the entropic elasticity of polymer networks with the orientational order of liquid-crystal mesogens, enabling large, reversible shape changes directly coupled to the nematic order parameter [20–24]. In both side-chain and main-chain architectures, the mesogens constitute the majority of the material's mass. In the case of side-chain LCEs, the nematic molecules are coupled to the polymer backbone, whereas main-chain LCEs incorporate the nematic molecules directly into the polymer chains. Through the two-step Finkelmann crosslinking process, an internal stress field is imprinted into the network, giving rise to giant thermomechanical (TM) contraction – often exceeding 100 % strain (defined as $\Delta l/l$) in main-chain systems [20,25–29].

Because mechanical stress couples directly to the nematic order parameter, LCEs can exhibit a measurable elastocaloric response upon stretching or releasing. Early direct measurements demonstrated that main-chain LCEs can produce elastocaloric temperature changes of ~0.4–1 K at stresses as low as 0.1–0.2 MPa, corresponding to elastocaloric responsivities of 4–25 K MPa^{-1}-two to three orders of magnitude larger than those of SMAs [27,28,30,31]. Subsequent studies showed that the magnitude and sharpness of the nematic – isotropic (N–I) transition, and thus the elastocaloric response, can be tuned by varying the crosslinking density. Lower crosslink densities shift the transition towards first-order behaviour, introduce latent heat, and significantly enhance both the TM and eC responses [27,28,32–35].

These findings position main-chain LCEs as highly promising candidates for low-stress, high responsivity elastocaloric cooling. However, for any caloric material to be viable in real-world devices, its long-term mechanical and functional stability under repeated cycling must be understood. While SMAs often suffer from fatigue and fracture under cyclic loading, LCEs – owing to their polymeric nature – may offer superior durability. Nevertheless, systematic studies of thermomechanical and elastocaloric ageing, including how repeated actuation influences the N–I transition, mesogen alignment, and eC performance, remain scarce [35].

In this work, we address this gap by investigating the long-term thermomechanical and elastocaloric stability of main-chain LCEs subjected to extensive cyclic stretching. Using monodomain samples with tunable crosslink densities, we examine how repeated actuation affects the N–I transition temperature, the magnitude of the elastocaloric response, and the structural integrity of the elastomer network. Our results reveal that main-chain liquid-crystalline elastomers maintain excellent mechanical resilience even after one million cycles, while exhibiting systematic and interpretable changes in both TM and eC behaviour. These insights highlight the robustness and tunability of LCEs and further support their potential as sustainable working materials for next-generation solid-state cooling technologies.

2. Sample preparation and experimental

2.1. Sample synthesis and preparation procedures

The main-chain liquid crystalline elastomers (MCLCEs) investigated in this study were synthesised using the conventional two-step Finkelmann crosslinking procedure, which reliably produces monodomain elastomers with strong, reproducible thermomechanical and elastocaloric responses [25,28]. As in related studies, mesogenic units are incorporated directly into the polymer backbone, forming the primary chain of the elastomer network with our custom synthesis [27,30]. The synthesis employed 1,1,3,3-tetramethyldisiloxane as a chain extender and 2,4,6,8,10-pentamethylcyclopentasiloxane as the crosslinker, with toluene serving as the solvent and dichloro(1,5-cyclooctadiene) platinum(II) in dichloromethane as the catalyst, following procedures consistent with previous MCLCE report [36]. The components are present in Figure 1(a–c).

In the first crosslinking stage, a weakly crosslinked elastomeric network was formed. The partially cured material was then uniaxially stretched in the nematic phase to impose orientational alignment of the mesogenic

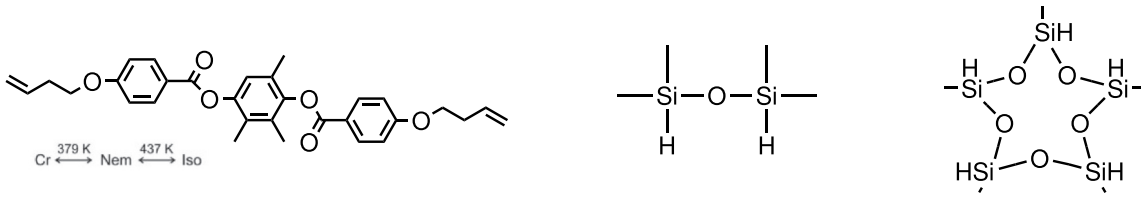

Figure 1. Chemical components of the MCLCE material: (a) Main-chain mesogenic monomer, (b) Polymer chain extender and (c) Five-points crosslinker.

units [25,26]. The second crosslinking step, performed at approximately 343 K, fixed this internal stress field and produced monodomain samples exhibiting thermomechanical strains exceeding 100 %, consistent with earlier observations in main-chain systems [20,27,28]. These elastomers displayed strong coupling between mechanical stress and mesogen orientation, making them ideal candidates for studying the interplay between microstructural tuning, ageing, and elastocaloric performance [24].

The synthesis was carried out under stoichiometric hydride – vinyl conditions and in a relatively dilute toluene solution, which was chosen to promote homogeneous network formation and high conversion of the reactive groups. Similar main-chain LCE syntheses based on controlled stoichiometry and end-linking have been reported [37–39] to yield high-gel-fraction networks, while gel fraction in LCEs is commonly quantified by solvent extraction/swelling followed by drying and weighing. In the present study, samples from various batches were used and showed no measurable differences in any of the measured quantities, indicating that soluble oligomers, if present, do not dominate the ageing behaviour discussed here.

Two compositions with molar crosslinker parts of $\phi = 0.05$ and 0.07, denoted MCLCE-5 and MCLCE-7, respectively, were synthesised to tune the character of the nematic – isotropic (N–I) transition from supercritical-like at high crosslinking density to a more critical one at low density, thereby modulating the sharpness of the transition and thus the elastocaloric responsivity [27,28]. Varying this parameter enables systematic tuning of the nematic – isotropic (N–I) phase transition character – from a continuous, supercritical regime at high crosslinking density to a sharp, first-order-like transition at low crosslinking density – thereby directly influencing both the latent heat and the elastocaloric response [32,33]. The N-I phase transition occurs at approximately 410 K. Rectangular specimens ($\approx 15 \times 3 \times 0.3$ mm^3) were used in this study. This geometry is standard for direct caloric measurements and ensures uniform strain distribution during uniaxial loading [27,28]. All samples were annealed above the N-I transition prior to measurements to remove residual stresses and ensure reproducible behaviour.

2.2. Experimental methods

All thermomechanical and elastocaloric measurements were performed using a custom-built extensometer, similar in design to those used in previous direct caloric studies on LCEs [27,30]. The setup consists of a temperature-controlled copper block that serves as a thermal bath. The temperature is controlled via a Lakeshore temperature controller 350 to a precision of 0.001 K. Above the chamber is a precision-driven stepper motor translator. Below the heated copper chamber is a strain gauge that measures tensile or compressive forces [22]. Furthermore, the sample can be equipped with a small 500 k Ω thermistor, wired to a Keithley 2002 multimeter that measures its resistance, thereby determining the sample's temperature. The sample is fixed between two holders, which are mounted to the strain gauge and translator motor, respectively.

For thermomechanical measurements, the sample was subjected to controlled heating and cooling cycles within the copper chamber while maintaining a constant preload tension, consistent with standard characterisation approaches in liquid-crystalline polymer networks [40]. The translator compensated for thermal length changes to maintain quasi-static conditions, while strain and temperature were continuously recorded. This procedure follows established protocols for characterising the temperature-dependent strain response of MCLCEs [26–28,30].

2.2.1. Elastocaloric measurements

Direct elastocaloric measurements were performed by applying a rapid uniaxial stretch at constant bath temperature, followed by a short hold period (15–20 s) to allow internal thermal equilibration and mechanical relaxation. The adiabatic temperature change ΔT_{eC} was extracted from the thermistor signal, while the applied stress was determined from the strain gauge output. This configuration enables simultaneous acquisition of mechanical and thermal data with millikelvin sensitivity and micrometre-level strain resolution, thereby providing direct characterisation of the elastocaloric response under near-adiabatic loading and unloading conditions, as in other caloric and mechanocaloric measurement methodologies [12,27,28,30,41,42]. To minimise heat exchange with the environment, samples were mounted in low-thermal-conductivity glass holders using Kapton tape, ensuring minimal thermal contact while maintaining mechanical stability. The mounting is pictured in Figure 2.

The measurement protocol was repeated at temperatures spanning the N–I transition to capture the peak elastocaloric response. The ageing was later performed at the N–I transition, i.e. the temperature at which the largest eC response is observed.

2.2.2. Ageing measurements

Ageing experiments were conducted in two stages. First, stress-relaxation measurements were performed by stretching the sample to a prescribed length (typically within 1 s) and holding it stretched for 60 seconds

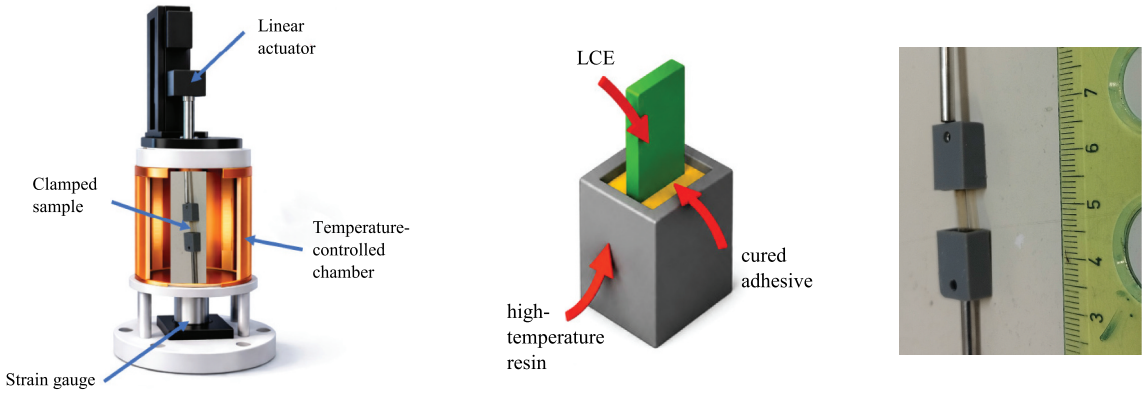

Figure 2. Homemade extensometer (left), sample mounting in loose plastic holder for ageing measurements, sketch (middle), and actual view with sample mounted (right).

(Figure 3), while monitoring the exponential decay of the required stress field to maintain the sample's stretch. The sample was extended length-wise as the director of the order parameter of the MC-LCE is in that same direction, optimising the applied filed for orientation of the polymeric backbones and hence the orientation of the nematic molecules. The stress field exhibits a peak immediately after the prescribed length is reached and then relaxes to the steady-state value with a characteristic time of about 1.5–2 seconds (see the inset to Figure 3). The stress-relaxation region was fitted after completion of the stretching ramp, during the constant-strain holding period. The ramp and unloading parts of the curve were excluded from the fit. The relaxation was described using a single-exponential decay with a non-zero stress offset, $\sigma(t_{\mathrm{rel}}) = \sigma_\infty + A\exp\left(-\frac{t_{\mathrm{rel}}}{\tau}\right)$ where t_{rel} is the time measured from the beginning of the constant-strain hold, σ_∞ is the relaxed stress plateau, A is the relaxation amplitude, and τ is the characteristic relaxation time. For the representative curve shown in Figure 3, the fit yielded $\sigma_\infty = 0.17849 \pm 0.00003$MPa, $A = 0.01374 \pm 0.00029$MPa, and $\tau = 2.15 \pm 0.07$s. This behaviour is consistent with the viscoelastic relaxation and softening dynamics reported in LCEs and related elastomer systems [27,30,43,44]. During the ageing measurements, the elastomers were cycled at a frequency of around 1.5 Hz, which is more relevant for real applications. Such a frequency is slightly faster than the characteristic relaxation time above would suggest. We argue that rapid cycling keeps the sample in a state of mechanical distress, in which the polymer backbone alternates between attempts to relax and restretching. This situation is likely harder for the MC-LCE to endure, as external and internal forces switch rapidly.

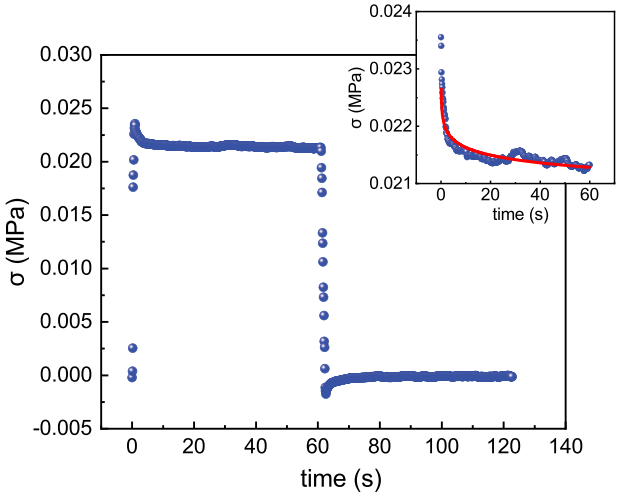

Figure 3. Stress σ as a function of time during a representative stress-relaxation measurement. The sample was rapidly stretched to the prescribed strain and then held at fixed length before unloading. The inset shows the relaxation region fitted with a single-exponential decay with a non-zero stress offset, yielding a characteristic relaxation time of $\tau = 2.15 \pm 0.07$s.

In the second stage, long-term cyclic loading was applied to evaluate mechanical durability and ageing-induced changes in caloric performance. Samples were cycled at 1.5 Hz between fixed strain limits, with total cycle counts ranging from 10^4 to 10^6 depending on crosslinking density. To prevent sample fracture at elevated temperatures, a compliant clamping system was developed: the sample ends were embedded in 3D-printed *Phrozen TR300* high-temperature resin cubes filled with cured adhesive, providing a soft mechanical interface that avoids stress concentration. Experiments with a variety of rigid-interface clamping systems resulted in the sample tearing or breaking after a few thousand cycles, always at the transition section between the rigidly clamped and free sections. Our clamping system is presented in Figure 2. Similar issues

with fracture susceptibility and fatigue sensitivity have been discussed in recent LCE fatigue-resistance studies [29,45,46]. The improved clamping method for the sample, which uses a rigid holder to hold the fragile sample softly, mediated by hardened glue, was used for both MCLCE samples with 5% and 7% crosslinking densities.

During cycling, the sample length at maximum and minimum extension was continuously monitored to detect gradual changes in network relaxation, creep, or permanent changes. After ageing, both TM and eC measurements were repeated to quantify shifts in the N–I transition temperature and changes in elastocaloric amplitude.

3. Results and discussion

3.1. Ageing of thermomechanical response

Firstly, some preliminary tests were carried out. For these, we used both MCLCE-5 and MCLCE-7 samples, employing relative strains of 15 % ($\lambda = 0.15$) and 10 % ($\lambda = 0.10$), respectively. These samples are close to the liquid-vapour type critical point [47] in the temperature – crosslinking density phase diagram [28] and were chosen as the softest at the N-I phase transition. The stretching and retracting cycles were carried out at a constant temperature near the N-I phase transition temperature, as the thermomechanical response at the N-I transition shows the strongest rise and eCE reaches its maximum [27,28,30]. A virgin sample, approximately 15 mm long, was used in both cases. Firstly, the spontaneous thermomechanical response initially occurs around the N-I phase transition temperature. In the case of MCLCE-7, within the first 3000 cycles, while employing a relative strain of 10 % ($\lambda = 0.1$), the shift of the N-I phase transition was monitored every 1000 cycles. Figure 4(a) shows the shift of the N-I transition as a function of the number of stretching cycles N. After completing 10,000 cycles, spontaneous thermomechanical response and N-I transition temperature were again determined, see Figure 4(b) for MCLCE-5. The amplitude of relative strain of $\lambda = 0.15$ was about two times larger than the spontaneous thermomechanical response at N-I transition temperature at which ageing was actually performed in MCLCE-5 (see Figure 4(b)).

Figure 4 shows a modest shift in the N-I transition temperature, $\Delta T_{NI} = 2.9$ K, after completing 10,000 stretching cycles with a tendency towards saturation. No reduction of the spontaneous thermomechanical response is observed for this small number of cycles (see Figure 4(b)), demonstrating preservation of mechanical elastomeric integrity.

As the MCLCE-5 sample is relatively close to the critical point and softer than MCLC-7, we decided to perform an extensive ageing study on the MCLCE-7 sample, which is more rigid but still shows a large eCE and an even larger thermomechanical response. Here, the relative strain amplitude was kept the same ($\lambda = 0.1$) as in the initial cycling for easier comparison. Still, it was about ≈25 % of spontaneous thermomechanical response at room temperature and about equal to the spontaneous thermomechanical response at N-I transition temperature (see Figure 5). The spontaneous thermomechanical strain, $\lambda(T)$, can be used as a functional proxy for changes in the orientational order and its coupling to the polymer network. In monodomain liquid-crystalline elastomers, changes in the nematic order parameter, $S(T)$, directly affect the anisotropy of the network-chain conformation and are

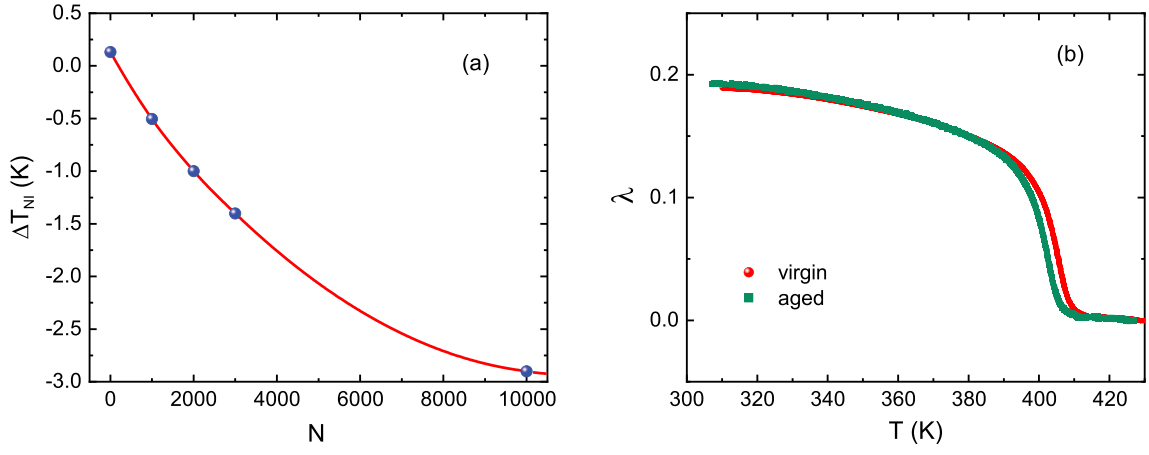

Figure 4. Shift of the N-I phase transition temperature ΔT_{IN} induced by mechanical cycling in the MCLCE-7 (a) and spontaneous thermomechanical relative strain λ measured in the virgin MCLCE-5 sample and after the completion of 10,000 stretching and retracting cycles (b).

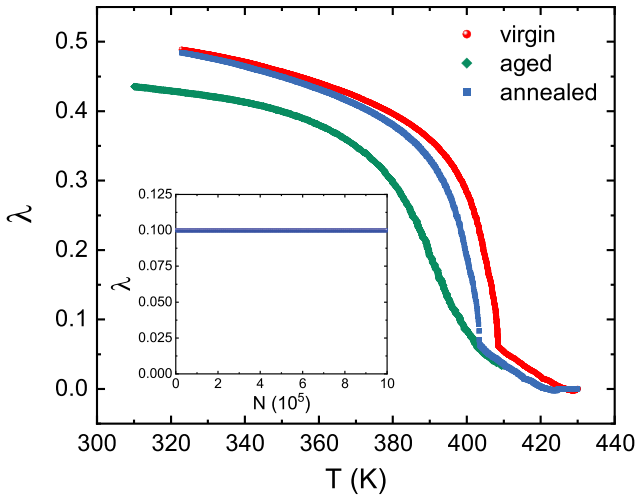

Figure 5. Thermomechanical response of a virgin MCLCE-7 sample (red circles), an aged sample (green diamonds), and a thermally annealed sample at 410 K for three weeks (blue boxes).

therefore expressed macroscopically as changes in $\lambda(T)$. For this reason, the temperature dependence of $\lambda(T)$ provides direct functional information on the evolution of order-related thermomechanical response during ageing. Consequently, while structural measurements such as WAXS/SAXS or NMR would provide additional microscopic information, they are not essential for identifying the ageing-induced changes relevant to the present study. Here, the shift and broadening of $\lambda(T)$, together with the evolution of stress and effective modulus, are therefore used as experimentally accessible indicators of changes in the strain – order coupling. Nevertheless, we do not assign these changes to a single microscopic mechanism in the absence of direct structural measurements [31,48].

Similarly to the MCLCE-5 sample, we initially measured the spontaneous TM response as a function of temperature on a virgin sample (red circles in Figure 5). It should be noted that the spontaneous TM response in the MCLCE-7 sample was about 2.5 times larger than in the MCLCE-5 sample. The sample was then subjected to a single large run of 1,000,000 stretching and retracting cycles with a stretching amplitude $\lambda = 0.1$ (inset of Figure 5), which took about three weeks to complete. After completion of 1,000,000 stretching cycles, the spontaneous thermomechanical response was measured again (green diamonds in Figure 5). A significant shift of the N-I transition temperature of $\approx$13 K was observed between these two curves. In addition, slight smearing of the N-I transition and a 12 % reduction in the spontaneous TM response were observed at 320 K in the aged sample. As the sample was aged for a very long time at a relatively high temperature (around 410 K), its thermal degradation could account for some of the observed changes. To test this possibility, another run was performed in which a virgin sample (from the same batch) was not mechanically stretched, but annealed (kept at) 410 K for three weeks (blue boxes in Figure 5). The annealing run showed a smaller shift in the N-I transition temperature of only 4.8 K, practically no smearing of the N-I transition, and only a minute reduction in the spontaneous TM response of 1 % at 320 K. The results demonstrate that one million cycles of mechanical stretching cause a small degradation of the sample, reducing the TM response by about 10 % and lowering and broadening the N–I transition temperature by approximately 2–3 %, effects that may not be solely attributable to thermochemical degradation. It is plausible that the oriented sample during fast, dynamically nonequilibrium mechanical stretching becomes slightly less oriented due to annealing of the second-stage crosslinking-imprinted internal stress field and partial rearrangement of the crosslinked network [49]. Such changes slightly modified the thermodynamic conditions for the phase transition. Similar network-relaxation-driven shifts in phase behaviour have been reported in recent analyses of LCE fatigue and fracture evolution [29,41,45,50]. High-temperature annealing likely relaxed internal stresses and reduced spatial heterogeneity in crosslink environments, allowing the transition to occur more cooperatively and therefore preserving sharpness, consistent with established understanding of thermally driven relaxation and reorganisation in liquid crystal polymer networks [40]. Ageing can weaken the effective coupling between mesogens and the elastomer backbone leading to altered network modulus, phenomena that are broadly consistent with recent analyses of fatigue, fracture, and microstructural softening in LCEs [29,44,45]. Each of these effects reduces the free-energy difference between the nematic and isotropic states, forcing the sample into a more relaxed steady state with a lower N-I transition temperature [42]. This would account for the smearing of the transition and TM reduction. Such TM reduction after cycling would also result in the stress field increase required for keeping the induced relative strain λ constant as well as the increase in the effective Young modulus $E = \sigma/\lambda$, both shown in Figures 6 and 7 for MCLCE-5 and MCLCE-7 samples, respectively. We speculate that in less crosslinked samples, there will be more reversible polymer network untangling than irreversible bond breaking, whereas in more crosslinked, more rigid samples, irreversible bond breaking will become dominant, leading to decreased TM (i.e. increased effective Young modulus). Indeed, experiments show that for a small number of cycles below

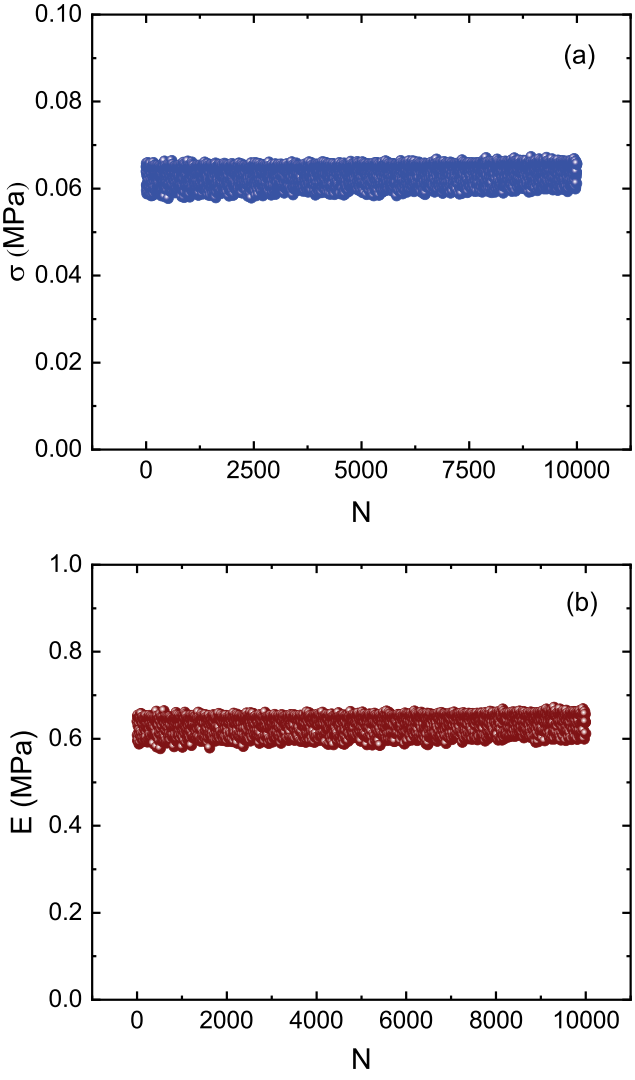

Figure 6. Stress field required for constant $\lambda = 0.15$ (a) and effective Young modulus E (b) as functions of number of stretching cycles N in MCLCE-5 sample.

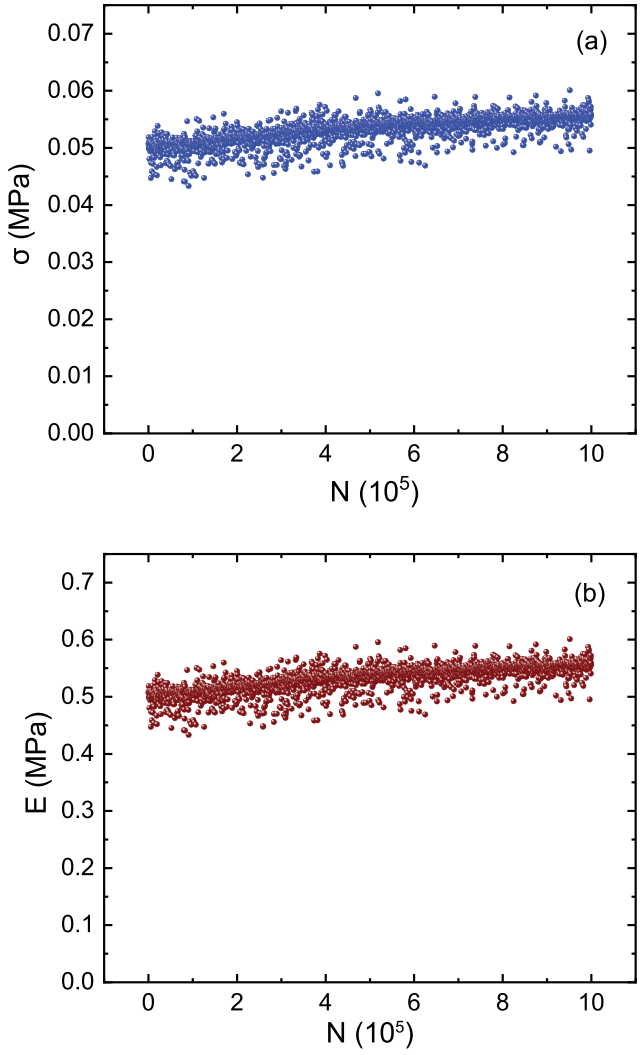

Figure 7. Stress field required for constant $\lambda = 0.10$ (a) and effective Young modulus E (b) as functions of number of stretching cycles N in MCLCE-7 sample.

10,000, no measurable change (<0.1 %) is observed in both σ and E (Figure 6) in a softer MCLCE-5 sample. In contrast, after 10,000 cycles, about 0.25 % change is observed in both quantities in the MCLCE-7 sample, which steadily increases with increasing N to about 12 % after 1,000,000 stretching cycles (Figure 7).

3.2. Ageing of elastocaloric response

Initial ageing experiments of the elastocaloric response were performed on both MCLCE-5 and MCLCE-7 samples, which are known to exhibit the largest enthalpy and sharpness of the N-I phase transition of the prepared samples and, consequently, the strongest elastocaloric response, making them particularly attractive for potential applications [28]. The ageing procedure was performed as described in the previous section, with up to 10,000 stretching cycles for the MCLCE-5 sample and up to 1,000,000 cycles for the MCLCE-7 sample. In addition, the elastocaloric change of temperature ΔT_{eC} was measured as a function of temperature in the vicinity of the N-I transition in the virgin samples and after every 1000 stretching cycles, up to the first 3000 cycles, and once more after 10,000 cycles in 5 % and after 1,000,000 cycles in 7 % samples, respectively. As shown in the previous section, the N-I transition shifts with the number of cycles, N. The ΔT_{eC} was therefore measured at several temperatures around the N-I transition to determine the maximum eCE response, i.e. the maximum of $\Delta T_{eC}(T)$ for a given N. For the elastocaloric measurements, the same amplitude of the relative strain of $\lambda = 0.10$ as in the case of TM ageing was applied in the case of the MCLCE-7 sample, and a slightly larger relative strain of $\lambda = 0.15$ was used

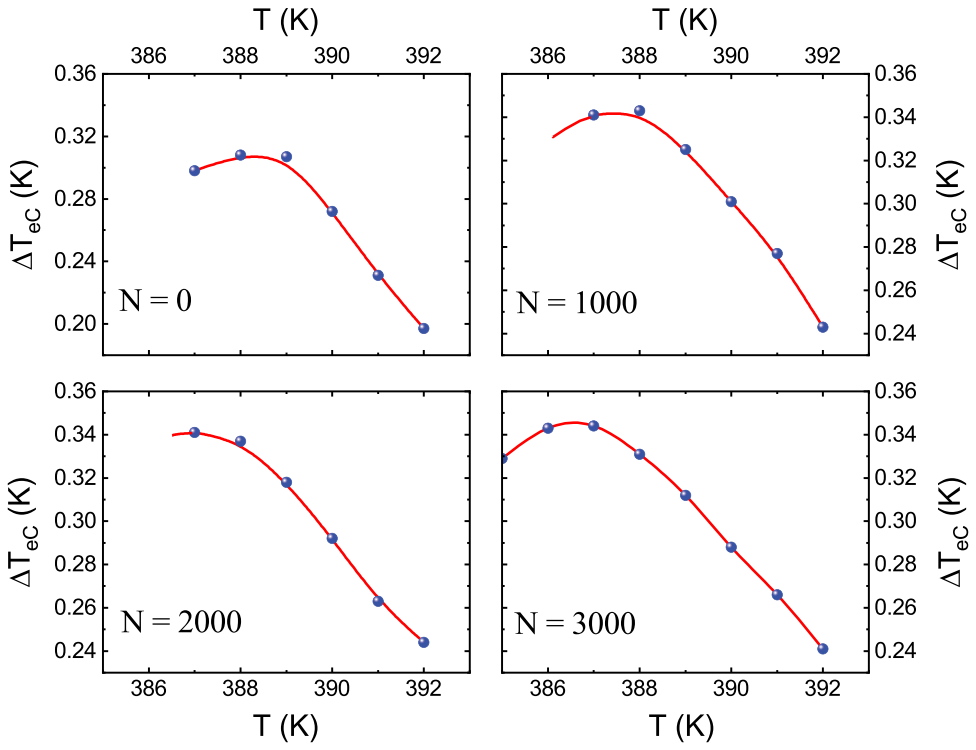

Figure 8. Elastocaloric change of temperature ΔT_{eC} as a function of temperature at different *N* for the MCLCE-7.

in the MCLCE-5 sample in order to maximise the observable temperature response and improve the signal-to-noise ratio.

Figure 8 shows a set of measurements of ΔT_{eC} versus temperature at different *N* for the MCLCE-7 sample. As the N-I phase transition shifts to lower temperatures with increasing number of cycles *N*, the peaks in ΔT_{eC} consistently shift to lower temperatures. The maximum peak value of ΔT_{eC} also exhibits a transitional effect, as shown in the left panel of Figure 9. Cycling increases the initial lower peak ΔT_{eC} value, which saturates within the first 1000 cycles to about 10 % higher value. This *transient* effect is likely due to internal stress annealing and increased mesogen ordering from repeated stretching. Such training-like evolution has been documented in elastomeric and caloric systems undergoing repeated loading, where microstructural reorganisation progressively enhances responsiveness [41,43]. This behaviour likely reflects a progressive reorientation and stabilisation of the mesogenic domains under repeated strain [44], leading to more efficient coupling between mechanical deformation and entropy change [40]. Together, these processes produce a more uniform but thermodynamically softened nematic network, consistent with the observed sharper, lower-temperature phase transition [44], thereby enhancing the elastocaloric effect.

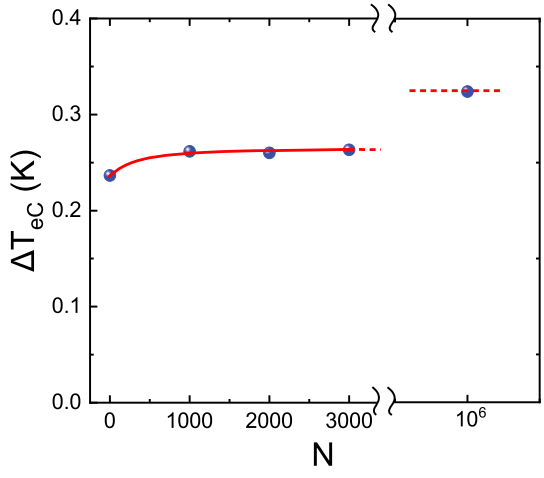

Figure 9. Elastocaloric change of temperature ΔT_{eC} as a function of the number of stretching and retracting cycles *N* for the MCLCE-7.

Such enhancement was especially visible in the already softer MCLCE-5 samples. Figure 10 shows the time evolution of the temperature after a constant relative strain of 0.15 is applied at $t = 0$. The ΔT_{eC} was determined after the removal of the strain, as the amplitude of the fast-cooling temperature (indicated by vertical lines with double arrows in Figure 10). Initial cycling in this soft MCLCE substantially increased ΔT_{eC} from 0.5 K in the virgin sample to 0.9 K after completing 10,000 stretching-retracting cycles. The

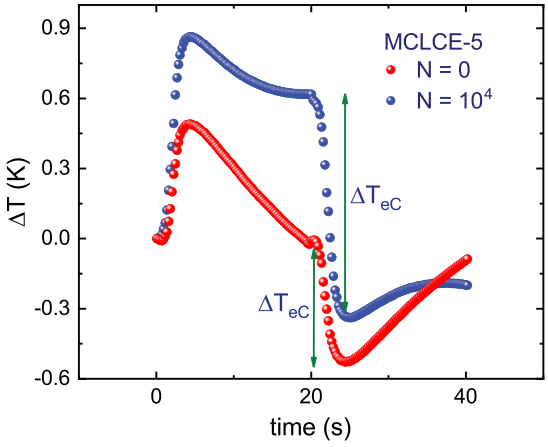

Figure 10. Elastocaloric change of temperature ΔT as a function of time within a single cycle measured in virgin ($N = 0$) MCLCE-5 and at $N = 10^4$.

combination of a reduced transition-temperature shift and an enhanced elastocaloric response suggests that mechanical cycling primarily modifies the coupling between strain and orientational order rather than significantly degrading the caloric functionality. Similarly to the above transient initial eCE enhancement, the saturated peak ΔT_{eC} value observed in the initial 3000 ageing cycles is gradually increased during further ageing cycling to about 23 % higher final value after completion of 1,000,000 stretching-retracting cycles (see right part of Figure 9). This slightly smaller increase in eCE than in the MCLCE-5 sample indicates that two competing mechanisms are at work. First, the ordering mechanism improves the coupling between strain and orientational order; the second mechanism has the same degrading ageing origin as described in the ageing of TM section. The first internal stress annealing mechanism, significantly improves eCE during initial cycling, while the second, degrading mechanism, such as hypothetical irreversible bond tearing resulting in weakening of the effective coupling between mesogens and the elastomer backbone, gradually reduces eCE. These degrading effects smear the N-I transition (compare TM curves in Figure 5), leading to a slight reduction of the eCE temperature change $\Delta T_{eC} \propto (\partial\lambda/\partial T)_{\sigma}$ [31]. It should be stressed that the first eCE-enhancing mechanism still prevails over the ageing mechanism even after 1,000,000 stretching-retracting cycles. This can be a consequence of the irreversible bond-tearing mechanism, which, though it decouples the mesogens from the elatomeric backbone, it also reduces imprinted disorder by reducing crosslinking points, thus allowing easier ordering under external force.

The similar darkening observed in the mechanically cycled and thermally annealed samples suggests that the colour change is primarily associated with prolonged thermal exposure rather than mechanical cycling. Such thermally induced discoloration has been reported in silicone/siloxane elastomers, where ageing temperature, oxidative environment, and platinum-complex residues can influence yellowing or browning, sometimes without a corresponding catastrophic loss of mechanical performance [51,52]. These observations collectively point to a mild 'training' effect, in which cyclic mechanical loading enhances elastocaloric efficiency while inducing a small, irreversible shift in the material's phase behaviour. Importantly, despite this visible alteration, small loss of mechanical and no significant loss of elastocaloric performance was detected, suggesting that the discolouration is a thermal-chemistry ageing effect with minimal influence on the functional properties of the material, consistent with reports of fatigue-resistant LCE architectures that maintain actuation or transition behaviour despite extended stress or environmental exposure [46].

4. Conclusion

The present study demonstrates that main-chain liquid-crystalline elastomers exhibit exceptional mechanical and functional stability under prolonged cyclic actuation, reinforcing their potential as durable elastocaloric materials for solid-state cooling applications. After one million stretch – retraction cycles, the samples retained their mechanical integrity without significant degradation, delamination, or loss of elasticity. Instead of fatigue-induced deterioration, an improvement in the elastocaloric effect was observed in MCLCE-5 by about 80 % after 10,000 cycles and in MCLCE-7 by 23 % after one million stretch – retraction cycles, likely arising from progressive alignment and relaxation of mesogenic domains within the polymer network. Furthermore, a downshift of the isotropic-nematic phase transition temperature by approximately 13 K and a reduction of the spontaneous thermomechanical response by about 10 % at room temperature were observed, suggesting subtle reorganisation and internal stress release in the crosslinked network. Despite this shift, the materials continued to exhibit a pronounced and reversible thermomechanical response, confirming the robustness of their elastocaloric performance. These results indicate that mechanical ageing through repeated actuation can serve as a form of 'mechanical annealing', enhancing mesogen alignment and improving thermal response consistency without compromising structural resilience over large numbers of mechanical cycles (>1 million). Overall, negligible eCE ageing effects and large elastocaloric responsivity $\Delta T_{eC}/\sigma > 20$ K/MPa [28] position MCLCEs as highly

promising candidates for long-lifetime, flexible, and environmentally friendly heat-management applications, where reliability and tunability are critical for practical caloric technology deployment.

Acknowledgments

We thank funding support by the Horizon Europe Framework Program Action HORIZON-MSCA-2022-SE-01-H-GREEN (No. 101130520), NATO Science for Peace and Security Program under grant SPS G5980 'FRAPCOM', and the Slovenian Research and Innovation Agency (applicative project L1-70060 and Young Researcher grant PR11225).

All authors agree to be accountable for all aspects of the work.

Author contributions

CRediT: **Matic Morgan:** Conceptualization, Data curation, Formal analysis, Investigation, Methodology, Software, Validation, Visualization, Writing – original draft, Writing – review & editing; **Andraž Rešetič:** Funding acquisition, Resources, Validation, Writing – review & editing; **Zdravko Kutnjak:** Conceptualization, Funding acquisition, Resources, Validation, Visualization, Writing – review & editing; **Brigita Rožič:** Conceptualization, Funding acquisition, Methodology, Project administration, Resources, Supervision, Validation, Visualization, Writing – review & editing.

Disclosure statement

No potential conflict of interest was reported by the author(s).

Funding

The work was supported by the Slovenian Research and Innovation Agency [P1-0125].

Methods

Figure 2 and the graphical abstract were created by the authors and subsequently subjected to AI-assisted graphical enhancement (ChatGPT) to improve visual aesthetics (e.g. colour vividness and 3D appearance). No AI-generated scientific content, data, or figure elements were introduced.

References

[1] Xie Z, Sebald G, Guyomar D. Comparison of elastocaloric effect of natural rubber with other caloric effects on difierent-scale cooling application cases. Appl Therm Eng. 2016;111:914–926.

[2] Moya X, Kar-Narayan S, Mathur N. Caloric materials near ferroic phase transitions. Nat Mater. 2014;13(5):439–450. doi: 10.1038/nmat3951

[3] Moya X, Defay E, Heine V, et al. Too cool to work. Nat Phys. 2015;11(3):202–205. doi: 10.1038/nphys3271

[4] Hu J, Mathur ND. Advances in ferroelectric and multiferroic materials. Adv Electron Mater. 2022;8(6):2200541. Available from: https://advanced.onlinelibrary.wiley.com/doi/abs/10.1002/aelm.202200541

[5] Mischenko A, Zhang Q, Scott J, et al. Giant electrocaloric effect in thin-film pbzr0.95ti0.05o3. Science. 2006;311(5765):1270–1271. doi: 10.1126/science.1123811

[6] Neese B, Chu B, Lu S, et al. Large electrocaloric effect in ferroelectric polymers near room temperature. Science. 2008;321(5890):821–823. doi: 10.1126/science.1159655

[7] Valant M. Electrocaloric materials for future solid-state refrigeration technologies. Prog Mater Sci. 2012;57(6):980–1009. doi: 10.1016/j.pmatsci.2012.02.001

[8] Kutnjak Z, Rožič B, Pirc R. Electrocaloric effect: theory, measurements, and applications. In: Wiley encyclopedia of electrical and electronics engineering. John Wiley & Sons, Ltd; 2015. p. 1–19. Available from: https://onlinelibrary.wiley.com/doi/abs/10.1002/047134608X.W8244

[9] Moya X, Mathur N. Caloric materials for cooling and heating. Science. 2020;370(6518):797–803. doi: 10.1126/science.abb0973

[10] Nair B, Usui T, Crossley S, et al. Large electrocaloric effects in oxide multilayer capacitors over a wide temperature range. Nature. 2019;575(7783):468–472. doi: 10.1038/s41586-019-1634-0

[11] Li J, Torello A, Kovacova V, et al. High cooling performance in a double-loop electrocaloric heat pump. Science. 2023;382(6672):801–805. doi: 10.1126/science.adi5477

[12] Tušek J, Engelbrecht K, Eriksen D, et al. A regenerative elastocaloric heat pump. Nat Energy. 2016;1(10):16134. doi: 10.1038/nenergy.2016.134

[13] Liu J, Zhao D, Li Y. Exploring magnetic elastocaloric materials for solid-state cooling. Shape Mem Superelasticity. 2017;3(3):192–198. doi: 10.1007/s40830-017-0118-z

[14] Kabirifar P, Trojer J, Brojan M, et al. From the elastocaloric effect towards an e–cient thermodynamic cycle. J Phys Energy. 2022;4(4):044009. doi: 10.1088/2515-7655/ac92a5

[15] Qian S, Catalini D, Muehlbauer J, et al. High-performance multimode elastocaloric cooling system. Science. 2023;380(6646):722–727. doi: 10.1126/science.adg7043

[16] Chen X, Zhu W, Rattner A, et al. A self-actuated electrocaloric polymer heat pump design exploiting the synergy of electrocaloric effect and electrostriction. J Phys Energy. 2023;5(2):024009. doi: 10.1088/2515-7655/acc278

[17] Herman JA, Hoang JD, White TJ. Elastocaloric response of isotropic liquid crystalline elastomers. Small. 2024;20(32):e2400786. doi: 10.1002/smll.202400786

[18] Pieczyska E, Gadaj S, Nowacki W, et al. Phase-transformation fronts evolution for stress- and strain-controlled tension tests in tini shape memory alloy. Exp Mech. 2006;46(4):531–542. doi: 10.1007/s11340-006-8351-y

[19] Schmidt M, Schuetze A, Seelecke S. Scientific test setup for investigation of shape memory alloy based elastocaloric cooling processes. Int J Refr. 2015;54:88–97.
[20] Warner M, Terentjev E. Liquid crystal elastomers. New York: Oxford University Press; 2007.
[21] Wim Hd J. Liquid crystal elastomers: materials and applications. Berlin, Heidelberg: Springer; 2012.
[22] Ohm C, Brehmer M, Zentel R. Liquid crystalline elastomers as actuators and sensors. Adv Mater. 2010;22 (31):3366–3387. doi: 10.1002/adma.200904059
[23] Varanytsia A, Nagai H, Urayama K, et al. Tunable lasing in cholesteric liquid crystal elastomers with accurate measurements of strain. Sci Rep. 2015;5(1):17739. doi: 10.1038/srep17739
[24] Terentjev EM. Liquid crystal elastomers: 30 years after. Macromolecules. 2025;58(6):2792–2806. doi: 10.1021/acs.macromol.4c01997
[25] Küpfer I, Finkelmann H. Nematic liquid single crystal elastomers. Makromol Chem, Rapid Commun. 1991;12 (12):717–726. doi: 10.1002/marc.1991.030121211
[26] Rešetič A, Milavec J, Zupančič B, et al. Polymer-dispersed liquid crystal elastomers. Nat Commun. 2016;7(1):13140. doi: 10.1038/ncomms13140
[27] Lavrič M, Derets N, Črešnar D, et al. Tunability of the elastocaloric response in main-chain liquid crystalline elastomers. Liquid Cryst. 2020;48(1):1–7.
[28] Črešnar D, Derets N, Trček M, et al. Caloric effects in liquid crystal-based soft materials. J Phys Energy. 2023;5(4):045004. doi: 10.1088/2515-7655/acf0ea
[29] Agrawal D, Dong G, Cai S. Enhancing thermo-mechanical properties of liquid crystal elastomers through chain entanglements. ACS Appl Mater Interface. 2025;17(20):30094–30102. doi: 10.1021/acsami.5c04077
[30] Trček M, Lavrič M, Cordoyiannis G, et al. Electrocaloric and elastocaloric effects in soft materials. J Phil Trans R Soc A. 2016;374(2074): 20150301. doi: 10.1098/rsta.2015.0301
[31] Črešnar D, Rožič B, Kutnjak Z, et al. Theoretical and experimental study of elastocaloric responses in liquid crystalline elastomers. J Mol Liq. 2024;413:126058. doi: 10.1016/j.molliq.2024.126058
[32] Cordoyiannis G, Lebar A, Zalar B, et al. Criticality controlled by cross-linking density in liquid single-crystal elastomers. Phys Rev Lett. 2007;99 (19):197801. doi: 10.1103/PhysRevLett.99.197801
[33] Cordoyiannis G, Lebar A, Rožič B, et al. Controlling the critical behavior of paranematic to nematic transition in main-chain liquid single-crystal elastomers. Macromolecules. 2009;42(6):2069–2073. doi: 10.1021/ma802049r
[34] Rožič B, Kosec M, Uršič H, et al. Influence of the critical point on the electrocaloric response of relaxor ferroelectrics. J Appl Phys. 2011;110(6):064118. doi: 10.1063/1.3641975
[35] Derets N, Domenici V, Rešetič A, et al. Thermomechanical response of liquid crystal elastomers: role of crosslinker density. Mater Res Express. 2024;11(2):25701. doi: 10.1088/2053-1591/ad2342
[36] Bobnar M, Derets N, Umerova S, et al. Polymer-dispersed liquid crystal elastomers as moldable shape-programmable material. Nat Commun. 2023;14 (1):764. doi: 10.1038/s41467-023-36426-y
[37] Burke KA, Rousseau IA, Mather PT. Reversible actuation in main-chain liquid crystalline elastomers with varying crosslink densities. Polymer. 2014;55 (23):5897–5907. doi: 10.1016/j.polymer.2014.06.088
[38] Donnio B, Wermter H, Finkelmann H. A simple and versatile synthetic route for the preparation of main-chain, liquid-crystalline elastomers. Macromolecules. 2000;33(21):7724–7729. doi: 10.1021/ma0002850
[39] Merkel DR, Traugutt NA, Visvanathan R, et al. Thermomechanical properties of monodomain nematic main-chain liquid crystal elastomers. Soft Matter. 2018;14(29):6024–6036. doi: 10.1039/C8SM01178H
[40] White T, Broer J, Dirk J. Programmable and adaptive mechanics with liquid crystal polymer networks and elastomers. Nat Mater. 2015;14(11):1087–1098. doi: 10.1038/nmat4433
[41] Sebald G, Xie Z, Guyomar D. Fatigue effect of elastocaloric properties in natural rubber. Phil Trans R Soc A. 2016;374(2074):20150302. doi: 10.1098/rsta.2015.0302
[42] Zhang S, Fu Y, Nie X, et al. Shearo-caloric effect enhances elastocaloric responses in polymer composites for solid-state cooling. Nat Commun. 2024;15 (1):6567. doi: 10.1038/s41467-024-50870-4
[43] Lu HF, Nie ZZ, Bisoyi HK, et al. An ultrahigh fatigue resistant liquid crystal elastomer-based material enabled by liquid metal. Sci China Mater. 2022; 65:1679–1686.
[44] Park S, Oh Y, Moon J, et al. Recent trends in continuum modeling of liquid crystal networks: a mini-review. Polymers. 2023;15(8):1904. doi: 10.3390/polym15081904
[45] Zhou Y, Wei C, Jin L. Fracture of liquid crystal elastomers. Proc Natl Acad Sci USA. 2025;122(38): e2510727122. doi: 10.1073/pnas.2510727122
[46] Wang M, Li X, Gai Y, et al. Dual-amide engineered blue phase liquid crystal elastomers: synergistic fatigue resistance, programmable mechanochromics and spatiotemporally encrypted photonics. Adv Mater. 2025;37 (37):e2506129. doi: 10.1002/adma.202506129
[47] Kutnjak Z, Petzelt J, Blinc R. The giant electromechanical response in ferroelectric relaxors as a critical phenomenon. Nature. 2006;441(7096):956–959. doi: 10.1038/nature04854
[48] Krause S, Zander F, Bergmann G, et al. Nematic main-chain elastomers: coupling and orientational behavior. Comptes Rendus Chimie. 2009;12(1):85–104.
[49] Martin Linares CP, Traugutt NA, Saed MO, et al. The effect of alignment on the rate-dependent behavior of a main-chain liquid crystal elastomer. Soft Matter. 2020;16(38):8782–8798. doi: 10.1039/D0SM00125B
[50] Hu M, Wang L, Wei Z, et al. Fracture and fatigue characteristics of monodomain and polydomain liquid crystal elastomers. Soft Matter. 2025;21(1):113–121. doi: 10.1039/D4SM01042F
[51] Antosik AK, Bednarczyk P, Czech Z. Aging of silicone pressure-sensitive adhesives. Polym Bull. 2018;75 (3):1141–1147. doi: 10.1007/s00289-017-2083-2
[52] Brounstein Z, Zhao J, Geller D, et al. Long-term thermal aging of modified sylgard 184 formulations. Polymers. 2021;13(18):3125. doi: 10.3390/polym13183125